

Optimizing the Earth-LISA “rendez-vous”

Fabrizio De Marchi^{1*}, Giuseppe Pucacco², Massimo Bassan²

¹ Department of Physics, Università di Trento and INFN, Sezione di Trento, I-38100 Povo

² Dipartimento di Fisica, Università di Roma “Tor Vergata” and INFN, Sezione di Roma Tor Vergata, I-00133 Roma

Abstract. We present a general survey of heliocentric LISA orbits, hoping it might help in the exercise of rescoping the mission. We try to semi-analytically optimize the orbital parameters in order to minimize the disturbances coming from the Earth-LISA interaction. In a set of numerical simulations we include non-autonomous perturbations and provide an estimate of Doppler shift and breathing as a function of the trailing angle.

PACS numbers: 04.80.nm, 95.10.Eg

1. Introduction

The LISA space experiment to detect low frequency gravitational waves has been for a long time a priority mission of space agencies, both in Europe and in the US. There has recently been an ample discussion on a possible scaled-down version of the LISA mission that, in order to meet tighter budget constraints, could be characterized by a shorter arm length L , a closer mean distance from the Earth (a smaller trailing angle) and maybe a 2-arms (4-links) configuration, giving up the third arm. In this case, it becomes natural to consider a right angle geometry as an alternative to the traditional, 60° , equilateral triangle.

Although other configurations are being evaluated by the ESA Concurrent Design Facility team, these triangular ‘constellations’ on heliocentric Earth-trailing orbits still remain the favorite choice. We focus our attention on the evaluation of the usual kinematic indicators of performance (arm flexing, breathing angles and Doppler shifts) when reducing both the size of the triangle and the Earth-LISA distance over the entire mission lifetime. As is well known, the interaction of LISA with the Earth is the major perturbation. The dominant effect is a parabolic drift characterized by a “rendez-vous” (RV) at which the distance between the constellation and the Earth is minimum. We investigate how additional perturbing effects influence the motion of LISA around the RV and how it is possible to optimize it.

We assume the following guidelines:

- Arm Length: $L=1$ Gm. We consider two configurations: the equilateral triangle (ET) with side L and an isosceles right triangle (IRT) with two equal arms of length L and the third one $L\sqrt{2}$ long.

* Corresponding author: fdemarchi@science.unitn.it

- Flexing: the spacecraft (S/C) relative velocity in the sensitive axis (rate of change of the arm length) causes a Doppler shift of the laser frequency. We set a maximum bandwidth of 20 MHz over a $1\mu\text{m}$ carrier, corresponding to $V/c < 6.5 \times 10^{-8}$, or $V < 20$ m/s. Note, for the sake of plot readability, that the Doppler shift (in MHz) has the same numerical value than the longitudinal velocity (in m/s).
- Breathing angle: The relative motion of S/C's also imposes a continuous adjustment of the angle between two beams departing from the same corner, in order to track the opposite spacecrafts; this fluctuation over the nominal angle (60° or 90°) is referred to as breathing angle (BA). We demand $\text{BA} < \pm 1.5^\circ$.
- Trailing angle (TA, also referred to as Lag Angle): LISA follows the Earth on a heliocentric circular orbit and TA is the angle between the constellation and the Earth as seen from the Sun. TA is a good indicator of the Earth-LISA distance, because the radial secular motion (away from the Sun) of the constellation is normally much smaller than the tangential (along the Earth orbit) one. We demand TA as small as possible, compatibly with the above requirements. In any case, initial conditions are chosen in such a way that over the mission lifetime, TA never exceeds 21° .
- Mission lifetime: 6 years.

The plan of the paper is as follows: we start recalling the simple models describing the interaction between Sun and LISA (Section 2) and Sun, Earth and LISA (Section 3). In Section 4 we describe an optimization method with the aim of an important reduction of flexing, breathing angles and Doppler shifts. We test this method first on the simplified Sun-Earth-LISA model and then on a more complete model including the real gravitational effects due to the dynamics of the Solar System. Finally, in Section 5 conclusions are drawn.

While graphs and details are given below, we anticipate here some results:

- As far as Doppler and breathing requirements are concerned, a short LISA can safely be put in an orbit much closer to Earth: $\text{TA} \approx 12^\circ$ at RV (the baseline design was 20°), or 31 Gm.
- Should we give up the third arm (keep only 4 optical links), a right angled triangle can be employed and performs at least as well as the usual equilateral triangle in several of the tests (Doppler, breathing, etc.) we carried on.

2. Keplerian orbits

We describe the interaction of LISA with the Earth in the framework of the Hill-Clohesy-Wiltshire (HCW) system [1, 2]. In this and next section, we will assume the Sun at rest in an inertial reference frame. The origin of the HCW frame rotates around the Sun on a circular reference orbit of radius R_0 and with orthogonal axes oriented as follows: x is directed radially opposite the Sun, y is in the direction tangent to the motion and z is perpendicular to the ecliptic. The time evolution of these orbits can be described with adequate precision using the post-epicyclic approximation in the HCW frame [3, 4].

2.1. Zero order approximation

Under the effect of the Sun only, at zeroth order, the equations of motion for a S/C in the rotating frame are

$$\begin{aligned}\ddot{x} - 2\omega\dot{y} - 3\omega^2x &= 0, \\ \ddot{y} + 2\omega\dot{x} &= 0, \\ \ddot{z} + \omega^2z &= 0,\end{aligned}\tag{1}$$

where $\omega = \sqrt{GM_\odot/R_0^3}$ is the mean motion and the most general solution is a combination of an ellipse in the xy plane and an oscillation in the z direction

$$\begin{aligned}x(t) &= 2\left(2x_0 + \frac{\dot{y}_0}{\omega}\right) - \left(2\frac{\dot{y}_0}{\omega} + 3x_0\right)\cos\omega t + \frac{\dot{x}_0}{\omega}\sin\omega t, \\ y(t) &= y_0 - 2\frac{\dot{x}_0}{\omega} - 3(\dot{y}_0 + 2\omega x_0)t + 2\frac{\dot{x}_0}{\omega}\cos\omega t + 2\left(2\frac{\dot{y}_0}{\omega} + 3x_0\right)\sin\omega t, \\ z(t) &= z_0\cos\omega t + \frac{\dot{z}_0}{\omega}\sin\omega t.\end{aligned}\tag{2}$$

The natural choice, in order to avoid drifts and offsets, is to set $\dot{y}_0 = -2\omega x_0$ and $\dot{x}_0 = \omega y_0/2$, so that the trajectory is reduced to a combination of simple oscillations along the three axes. Moreover, for a rigid, polygonal constellation, the distance of the S/C from the origin must be constant, say h , so that we obtain [5]

$$\dot{z}_0 = \pm\frac{\sqrt{3}}{2}\omega y_0; \quad z_0 = \pm\sqrt{3}x_0; \quad y_0 = \pm\sqrt{h^2 - 4x_0^2}; \quad x_0 = \pm\frac{h}{2}.$$

The orbit of one of the S/C's in the HCW frame is a circular motion with constant angular velocity ω and radius h around the origin in a plane inclined of $\pm 60^\circ$ with respect to the xy (ecliptic) plane. A second S/C, describing the same path (with a certain delay), will be at a constant distance ℓ , from the first one. For n such S/Cs, on the vertices of a regular polygon, their distance h from the origin and the relative phase delay are

$$h = \frac{\ell}{2\sin(\pi/n)}, \quad \phi = \frac{2\pi}{n}.$$

Finally, we put $x_0 = \ell/2$ to be consistent with the notations of [6, 3] and the zero-order orbits turn out to be

$$\mathbf{r}_k^{(0)}(t) = \frac{\ell}{2\sin(\pi/n)} \left[\frac{1}{2}\cos\sigma_k, \sin\sigma_k, \frac{\sqrt{3}}{2}\cos\sigma_k \right], \quad \sigma_k = \frac{2\pi(k-1)}{n} - \omega t.\tag{3}$$

The ET constellation is obtained with $n = 3$ and $k = 1, 2, 3$, while the IRT one corresponds to $n = 4$ (and $k = 1, 2, 3$), namely

$$\mathbf{r}_k^{(0)}(t) = \frac{\ell}{\sqrt{2}} \left[\frac{1}{2}\cos\sigma_k, \sin\sigma_k, \frac{\sqrt{3}}{2}\cos\sigma_k \right], \quad \sigma_k = (k-1)\frac{\pi}{2} - \omega t.$$

2.2. First order approximation

A first optimization is possible by changing the tilt angle of the constellation, i.e. the inclination of the triangle with respect to the ecliptic. Introducing a parameter δ_1 [3] such that:

$$\pm 60^\circ + \delta_1 \frac{\ell}{2R_0}.$$

the first order corrections

$$\mathbf{r}_k^{(1)}(t) = (x_k^{(1)}, y_k^{(1)}, z_k^{(1)}), \quad (4)$$

are:

$$\begin{aligned} x_k^{(1)}(t) &= \frac{h^2}{2R_0} \left[\frac{3}{2} \left(\frac{1}{2} - \delta_1 \right) \cos \sigma_k - \frac{1}{8} \cos \sigma_k - \frac{5}{8} \right], \\ y_k^{(1)}(t) &= \frac{h^2}{2R_0} \left[\left(\frac{3}{2} - 3\delta_1 \right) \sin \sigma_k - \frac{1}{2} \sin 2\sigma_k \right], \\ z_k^{(1)}(t) &= \frac{h^2}{2R_0} \left[\frac{\sqrt{3}}{2} (\delta_1 - 1) \cos \sigma_k - \frac{1}{4} \sqrt{3} \cos 2\sigma_k + \frac{3\sqrt{3}}{4} \right]. \end{aligned} \quad (5)$$

where $h = \ell/\sqrt{3}$ for the ET configuration and $h = \ell/\sqrt{2}$ for the IRT. It can be shown [3] that, due to the small eccentricity and inclination of the orbits, the solution given by the above zero and first order terms differs from the exact Keplerian solution by less than 0.03% making the method of analytical series expansion a useful basis for an analytical model of the motions of LISA.

Choosing $\delta_1 = 5/8$, the first order (Keplerian) flexing is minimized in both ET and IRT configurations, giving, with arm lengths of order 1 Gm, an extra angle of respectively $7'$ and $4'$. Table 1 reports some orbit indicators (flexing, breathing angles, and Doppler shifts) relative to both IRT and ET configurations for $\delta_1 = 0$ and $\delta_1 = 5/8$. The indicators Δ^+ and Δ^- represent the difference between the maximum and minimum (respectively) value and the *nominal* value of a given parameter, over the 6 years of the mission.

3. The Earth effect

We now include the perturbation due to the Earth.

In the analytic approach the Earth is assumed at rest in the Hill frame. As shown in [6], in the *rotating frame*, the global dynamics in the coupled fields of Sun and Earth is characterized by secular terms producing, in the long run, a drift *away* from the Earth: this is linear in time in the radial direction and quadratic in the tangential direction.

In order to minimize this quadratic y drift, an intuitive strategy is to choose initial conditions such that LISA is a little further out at start, approaches the Earth, reaches its minimum distance at mid mission and departs after that [7]. However, other strategies can be devised that provide better performance of the constellation. An appreciable reduction of the flexing due to the Earth tidal field is in any case possible, over a limited time span, by suitable tuning of all orbital parameters [8, 9, 10]. In our analytical approach, in order to keep things simple, we still use three identical orbits (apart for relative phase shifts, see (3)) for the 3 S/Cs of the constellation and,

Table 1: Change of the relevant orbit indicators (arm length, breathing, Doppler modulation) for the three S/C's, for both IRT and ET configurations, in the standard $\delta_1 = 0$ and modified $\delta_1 = 5/8$ inclination. For each indicator, nominal value, average and deviations Δ^+ and Δ^- (see Section 2.2), relative to the nominal value over a mission lifetime of 6 years are shown.

$\delta_1 = 0$	IRT				ET			
	nominal	mean	Δ^+	Δ^-	nominal	mean	Δ^+	Δ^-
L_{12} [km]	10^6	1001333	+5210	-969	10^6	1001088	+3852	-757
L_{23} [km]	10^6	1001333	+5210	-969	10^6	1001088	+3859	-752
L_{31} [km]	$\sqrt{2} 10^6$	1416098	+4988	-1248	10^6	1001088	+3852	-757
θ_1 [deg]	45				60	60.00	+0.27	-0.18
θ_2 [deg]	90	90.00	+0.36	-0.26	60	60.00	+0.27	-0.18
θ_3 [deg]	45				60	60.00	+0.27	-0.18
$\Delta \mathbf{v}_{12}$ [m/s]	-	-0.11	+5.00	-5.16	-	0.00	+0.87	-0.87
$\Delta \mathbf{v}_{23}$ [m/s]	-	+0.16	+5.00	-4.55	-	0.00	+0.87	-0.87
$\Delta \mathbf{v}_{31}$ [m/s]	-				-	0.00	+0.87	-0.87

$\delta_1 = 5/8$	IRT				ET			
	nominal	mean	Δ^+	Δ^-	nominal	mean	Δ^+	Δ^-
L_{12} [km]	10^6	999115	+786	-2554	10^6	999277	+241	-1686
L_{23} [km]	10^6	999115	+786	-2554	10^6	999277	+241	-1686
L_{31} [km]	$\sqrt{2} 10^6$	1412962	-1251	-1253	10^6	999277	+241	-1686
θ_1 [deg]	45				60	60.00	+0.09	-0.09
θ_2 [deg]	90	90.00	+0.12	-0.12	60	60.00	+0.09	-0.09
θ_3 [deg]	45				60	60.00	+0.09	-0.09
$\Delta \mathbf{v}_{12}$ [m/s]	-	0.00	+0.27	-0.27	-	0.00	+0.16	-0.16
$\Delta \mathbf{v}_{23}$ [m/s]	-	0.00	+0.27	-0.27	-	0.00	+0.16	-0.16
$\Delta \mathbf{v}_{31}$ [m/s]	-				-	0.00	+0.16	-0.16

in addition to the above specs, we try and vary the tilt-angle δ_1 and a subset of the initial conditions. We first consider a simplified model where the Earth describes a circular orbit of radius $R_0 = 1\text{AU}$ around the Sun on the xy plane [11, 6]. Introducing the minimum trailing angle TA_0 , taking place at time t_0 , the Earth coordinates $(x_\oplus, y_\oplus, z_\oplus)$ in the HCW frame are

$$x_\oplus = -R_0(1 - \cos(\text{TA}_0)), \quad y_\oplus = R_0 \sin(\text{TA}_0), \quad z_\oplus = 0.$$

We consider its effect as a *constant + linear* force to be added to the equations of motion. We define the distance of the Earth from the origin, $d_\oplus = \sqrt{x_\oplus^2 + y_\oplus^2}$, and introduce the perturbation parameter

$$\varepsilon_\oplus = \frac{M_\oplus}{M_\odot} \left(\frac{R_0}{d_\oplus} \right)^3, \quad \frac{M_\oplus}{M_\odot} = \frac{1}{328900} \quad (6)$$

so that the effect of the Earth is given by the perturbation

$$\begin{aligned} f_{\oplus x} &= \varepsilon_{\oplus} \omega^2 (x_{\oplus} + C_{11}x + C_{12}y) \\ f_{\oplus y} &= \varepsilon_{\oplus} \omega^2 (y_{\oplus} + C_{12}x + C_{22}y) \\ f_{\oplus z} &= \varepsilon_{\oplus} \omega^2 (z_{\oplus} - z), \end{aligned}$$

where

$$C_{11} = \frac{2x_{\oplus}^2 - y_{\oplus}^2}{d_{\oplus}^2}, \quad C_{12} = \frac{3x_{\oplus}y_{\oplus}}{d_{\oplus}^2}, \quad C_{22} = \frac{2y_{\oplus}^2 - x_{\oplus}^2}{d_{\oplus}^2}. \quad (7)$$

The equations of motion can be solved with the perturbation method and the solutions, to be added to the zero and first order solutions, are in the form

$$\begin{aligned} x_k^{(E)}(t) &= (A_{k,x} + B_{k,x}t) \sin \omega t + (C_{k,x} + D_{k,x}t) \cos \omega t + E_{k,x} + F_x t, \\ y_k^{(E)}(t) &= (A_{k,y} + B_{k,y}t) \sin \omega t + (C_{k,y} + D_{k,y}t) \cos \omega t + E_{k,y} + F_{k,y}t + G_y t^2, \quad (8) \\ z_k^{(E)}(t) &= (A_{k,z} + B_{k,z}t) \sin \omega t + (C_{k,z} + D_{k,z}t) \cos \omega t. \end{aligned}$$

The integration constants $A_i \dots G_y$ are defined by the choice of initial conditions (see Appendix A). The secular terms appearing in the solution generate the parabolic drift around the RV (see Appendix B).

By collecting terms, the orbit of the S/C_k is

$$\mathbf{r}_k(t) = \mathbf{r}_k^{(0)}(t) + \mathbf{r}_k^{(1)}(t) + \mathbf{r}_k^{(E)}(t) \quad (9)$$

where the zero and first order terms are respectively given by (3) and (4) and $\mathbf{r}_k^{(E)}(t)$ is given by (8). The terms growing as t and t^2 in (respectively) $x^{(E)}(t)$ and $y^{(E)}(t)$ vanish when one calculates the relative motion between S/Cs, being F_x and G_y equal for all S/Cs, therefore the increase in flexing with time is only due to secular terms as $t \sin t$ and $t \cos t$.

It is now useful to define some quantities in the heliocentric frame:

- unit vectors of the rotating frame axes:

$$\begin{aligned} \mathbf{u}_x &= \{\cos(\omega t - \text{TA}_0), \sin(\omega t - \text{TA}_0), 0\}, \\ \mathbf{u}_y &= \{-\sin(\omega t - \text{TA}_0), \cos(\omega t - \text{TA}_0), 0\}, \\ \mathbf{u}_z &= \{0, 0, 1\} \end{aligned}$$
- Position of the Earth: $\mathbf{R}_{\oplus}(t) = R_0 \{\cos \omega t, \sin \omega t, 0\}$.
- Orbit of S/C_k:

$$\mathbf{R}_k(t) = (R_0 + x_k(t))\mathbf{u}_x + y_k(t)\mathbf{u}_y + z_k(t)\mathbf{u}_z \quad (10)$$
- LISA barycenter position: $\mathbf{R}_g(t) = \frac{1}{3} \sum_k \mathbf{R}_k(t)$.
- LISA arm vectors: $\mathbf{R}_{ij}(t) = \mathbf{r}_{ij}(t) = \mathbf{r}_j(t) - \mathbf{r}_i(t)$.
- LISA arm lengths: $L_{ij}(t) = |\mathbf{r}_{ij}(t)| = |\mathbf{R}_j(t) - \mathbf{R}_i(t)|$.
- Doppler shifts: $v_{ij}(t) = \frac{d}{dt} L_{ij}(t)$
- Trailing angle:

$$\text{TA}(t) = \frac{180}{\pi} \arccos \left(\frac{\mathbf{R}_{\oplus}(t) \cdot \mathbf{R}_g(t)}{R_0 R_g(t)} \right).$$

- Breathing angles:

$$\theta_j(t) = \frac{180}{\pi} \arccos \left(\frac{\mathbf{r}_{ij}(t) \cdot \mathbf{r}_{jk}(t)}{L_{ij}(t) L_{jk}(t)} \right)$$

4. Minimization of the flexing

We shall address the choice of an orbit that minimizes the flexing of the arms in three steps: first, by optimizing with respect to the tilt angle only. Then, by perturbing the initial conditions of the three S/Cs in a still analytic approach. Finally, with a fully numerical integration of the S/C orbits, taking into account all major perturbing effects. The mission begins at the time t_{ini} and is assumed to last $\Delta t = 6$ years. We refer to "mid-mission" or $t_{mid} = t_{ini} + 3$ yrs the time half way into the mission.

In the panels of Figure 1 we consider both the ET (red) and the IRT (blue) configurations: for these plots the optimization is only done by evaluating the optimal tilt-angle over the mission lifetime of 6 years. Optimization is performed by minimizing the RMS flexing of the 3 arms over the entire mission duration. The time of closest approach to the Earth is 3 years after the mission starts and this identifies TA_0 .

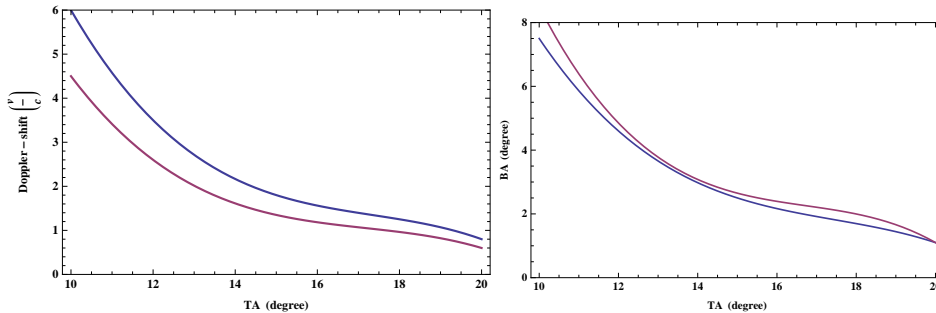


Figure 1: Effect of the Earth (non optimized): left: maximum Doppler shift in m/s . Right: maximum change of the angle between L_{12} and L_{13} (short arms in the IRT). Red curves: ET, blue curves: IRT.

The requirement of 6.5×10^{-8} on the Doppler shift shows that we can reduce the minimum TA to less than 10° for both cases (8° for the IRT). By choosing an optimal tilt angle we can strongly reduce the rms flexing of the arms; this angle always turns out to slightly differ from the canonical 60° . On the other hand, the breathing angle requirement of $\pm 1.5^\circ$ sets a limit at $TA \simeq 14^\circ$. Breathing appears therefore the major obstacle to an appreciable reduction of TA. In the next subsection, we attempt a more general optimization strategy.

4.1. Cost function

In order to extend the optimization to a wider set of parameters, we need to introduce a "cost function", i.e. a suitable function of the relevant quantities (the flexings) that has to be minimized. To this purpose, we define the following cost function, suitable for both configurations (and therefore different from those proposed in [8]):

$$\sigma^2 = \langle (L_{12} - \langle L_{12} \rangle)^2 + (L_{23} - \langle L_{23} \rangle)^2 + (L_{31} - \langle L_{31} \rangle)^2 \rangle \quad (11)$$

where

$$\langle \dots \rangle = \frac{1}{\Delta t} \int_{t_{ini}}^{t_{fin}} \dots dt.$$

indicates average over the mission time. Although in the IRT case the third arm is not monitored and its flexing could appear as a useless burden to the cost function, we maintained the same σ^2 , as defined in (11), for both configurations: minimizing the flexing of all arms is a way to render the triangle "more rigid" and is an effective strategy, as we shall show, to minimize the angle breathing as well.

4.2. Perturbation of initial conditions - semi-analytic approach

As we extend our optimization strategy, remaining as close as possible to an analytic approach, we must restrict the space of free parameters. Our choice is a subset of the initial conditions of the unperturbed orbits. The Earth produces linear and secular terms in the orbits, as shown by (8). On the other hand, (2) show that, in general, a linear drift exists in the y component (that we canceled by setting $2\omega x_0 + \dot{y}_0 = 0$). We can therefore choose a suitable offset in the initial conditions in such a way that these two linear drifts compensate each other.

Therefore, if we set

$$x_{0,k} = -\frac{\dot{y}_{0,k}}{2\omega} + \epsilon_k, \quad k = 1, 2, 3 \quad (12)$$

the first two components of position vector (3) become

$$\begin{aligned} x_k^{(0)} &= \frac{\ell}{2 \sin(\pi/n)} \frac{1}{2} \cos \sigma_k + \epsilon_k (4 - 3 \cos \omega t), \\ y_k^{(0)} &= \frac{\ell}{2 \sin(\pi/n)} \sin \sigma_k - 6\epsilon_k (\omega t - \sin \omega t) \end{aligned} \quad (13)$$

while the third one is unchanged.

In this way trajectories and arm-lengths are affected by a perturbation which grows linearly in time. In the expansion (9) we modify only the zero-order terms: in principle, the variation should be propagated through the higher-order terms, but the contribution is of order ℓ/R in the first-order terms and even smaller in the term describing the Earth effect: we can therefore safely neglect them.

The required amount of this variation can be determined by minimizing the cost function $\sigma^2(\epsilon_1, \epsilon_2, \epsilon_3, \delta_1)$ defined in (11). However, the analytic expression for σ^2 is sufficiently cumbersome to impose a numerical minimization: this, on the other hand, allows us to use the exact equations of motion:

$$\begin{aligned} \ddot{x}_k - 2\omega\dot{y}_k - \omega^2(x_k + R_0) &= f_{x,k} \\ \ddot{y}_k + 2\omega\dot{x}_k - \omega^2 y_k &= f_{y,k} \\ \ddot{z}_k &= f_{z,k} \end{aligned} \quad (14)$$

where \mathbf{f}_k is the Sun+Earth force per unit mass acting on the k -th S/C, expressed in the HCW coordinate system.

Setting the RV at $t_0 = t_{mid}$, for the IRT and ET configurations respectively, the minima correspond to

$$\begin{aligned} \text{IRT} : \quad \delta_1 &= 0.808, \quad \epsilon_1 = 867 \text{ km}, \quad \epsilon_2 = 519 \text{ km}, \quad \epsilon_3 = 66 \text{ km}, \\ \text{ET} : \quad \delta_1 &= 0.894, \quad \epsilon_1 = 523 \text{ km}, \quad \epsilon_2 = 64 \text{ km}, \quad \epsilon_3 = 7 \text{ km}. \end{aligned} \quad (15)$$

Table 2: Variation of the same orbital indicators as in Table 1 (arm-length, breathing, Doppler modulation) including the Earth effect (assumed on a circular orbit) corresponding to the optimal data of (15) for the IRT and ET constellations (left and right, respectively).

not opt.	IRT				ET			
	nominal	mean	Δ^+	Δ^-	nominal	mean	Δ^+	Δ^-
L_{12} [km]	10^6	1004681	+47356	-32740	10^6	1005887	+54846	-36195
L_{23} [km]	10^6	1005025	+55742	-42716	10^6	1001830	+16574	-16501
L_{31} [km]	$\sqrt{2} 10^6$	1425000	+92213	-59335	10^6	1006176	+59722	-40762
θ_1 [deg]					60	59.73	+2.71	-3.50
θ_2 [deg]	90	90.30	+4.27	-2.89	60	60.14	+3.91	-3.48
θ_3 [deg]					60	60.11	+4.00	-3.48
$\Delta \mathbf{v}_{12}$ [m/s]	-	-0.36	+8.76	-12.15		-0.30	+10.93	-13.95
$\Delta \mathbf{v}_{23}$ [m/s]	-	+0.49	+13.07	-10.17		+0.06	+5.62	-5.04
$\Delta \mathbf{v}_{31}$ [m/s]						+0.43	+14.72	-12.79
optimized	nominal	mean	Δ^+	Δ^-	nominal	mean	Δ^+	Δ^-
L_{12} [km]	10^6	999363	+14322	-16976	10^6	999440	+13569	-16262
L_{23} [km]	10^6	999284	+14665	-15256	10^6	999228	+12924	-15261
L_{31} [km]	$\sqrt{2} 10^6$	1413390	+18695	-21444	10^6	999353	+12793	-15472
θ_1 [deg]					60	59.99	+1.15	-1.16
θ_2 [deg]	90	90.01	+1.48	-1.50	60	60.00	+1.19	-1.24
θ_3 [deg]					60	60.01	+1.27	-1.26
$\Delta \mathbf{v}_{12}$ [m/s]	-	-0.11	+5.00	-5.16	-	-0.08	+4.88	-5.14
$\Delta \mathbf{v}_{23}$ [m/s]	-	+0.16	+5.00	-4.55	-	+0.01	+5.02	-5.05
$\Delta \mathbf{v}_{31}$ [m/s]					-	+0.14	+4.97	-4.69

The results of the optimization are reported in Table 2. The trailing angles in both cases at t_{ini} and t_{fin} are 12.8° degrees (33 Gm from the Earth). The improvement in the values of the performance indicators in the optimized cases is quite evident.

4.3. Numerical optimization

In this section we describe the fully numeric evaluation and minimization of the cost function (11) by solving the exact equations of motion and taking into account perturbing effect of the Sun, Venus, Earth, Moon, Mars and Jupiter. Their real trajectories $\mathcal{R}_\odot(t)$, $\mathcal{R}_\oplus(t)$, $\mathcal{R}_\text{J}(t)$, $\mathcal{R}_\text{V}(t)$, $\mathcal{R}_\text{M}(t)$, $\mathcal{R}_\text{Mars}(t)$ in the Solar System Barycenter (SSB), are provided by the JPL HORIZON ephemerides [12], with the following characteristics:

- Reference epoch: J2000.0
- XY-plane: plane of the Earth's orbit at the reference epoch.
- X-axis: out along ascending node of instantaneous plane of the Earth's orbit and the Earth's mean equator at the reference epoch.

- Z -axis: perpendicular to the XY -plane in the directional (+ or -) sense of Earth's north pole at the reference epoch.
- step: 1 day.

In the simplified model used till here, the Sun is assumed at rest at the center of an inertial frame. However, the true inertial frame is represented by the Solar System Barycenter (SSB), where the Sun moves in a non negligible and complex (non simply periodic) way: in this frame the motion of the Earth is substantially different from an ellipse, and therefore the initial condition that we adopted for the S/Cs using (2) are no longer suitable. Moreover, the motion of the Sun is also a relevant source of perturbation. Therefore, to account for these additional effects while maintaining the convenient, Sun-centered HCW description, we must complete the equations of motion with an apparent force deriving from the acceleration of the Sun relative to the SBB.

The equations of motion are as (14), with the forcing term modified as follows

$$f_{x,k} = (\mathbf{f}_k - \ddot{\mathcal{R}}_{\odot}) \cdot \mathbf{u}_x, \quad f_{y,k} = (\mathbf{f}_k - \ddot{\mathcal{R}}_{\odot}) \cdot \mathbf{u}_y, \quad f_{z,k} = (\mathbf{f}_k - \ddot{\mathcal{R}}_{\odot}) \cdot \mathbf{u}_z.$$

where \mathbf{f}_k is the total Newtonian force per unit mass on the k -th S/C.

$$\mathbf{f}_k = - \sum_{\alpha} \frac{GM_{\alpha}}{\|\mathcal{R}_{\odot} - \mathcal{R}_{\alpha} + \mathbf{R}_k\|^3} (\mathcal{R}_{\odot} - \mathcal{R}_{\alpha} + \mathbf{R}_k), \quad \alpha = \odot, \varphi, \oplus, \mathfrak{D}, \sigma, \mathfrak{I}. \quad (16)$$

and \mathbf{R}_k is the position of k -th S/C in the heliocentric frame (given by (10)).

The amplitude of flexing and breathing scales inversely with the LISA-Earth distance. This can be intuitively explained as follows: a small flexing is obtained if the constellation rapidly moves away from the Earth, its main source of perturbation to a rigid configuration. However, the overall distance in the mission lifetime must be bound within reasonable values dictated by communication requirements.

An analytical study of the evolution of the Earth-LISA distance is shown in Appendix B where it is verified that the LISA-Earth distance increases as t^2 , after (and before) the RV. Moreover, there is an additional sinusoidal modulation at 1 year period due to the eccentricity of the Earth's orbit. We prove that the minima of the sinusoid occur at well defined epochs that depend on the allowed minimum TA but not on the epoch t_0 of the RV. Therefore, in order to minimize the Earth-LISA distance, the optimal choice for t_0 is just one of these minima (B.5). This shows, as mentioned in Section 3, that other choices of t_0 , different from t_{mid} , can minimize flexing and breathing.

In the following we shall discuss two cases: $t_0 = t_{ini}$ and $t_0 = t_{mid}$. The value of TA_0 is chosen as the minimum one that allows a breathing angle smaller than 1.5° , as required. For the two configurations and the two kinds of RV considered the minima of the cost function is found at the following values of parameters:

IRT - RV at the beginning, ($t_0 = t_{ini}$):

$$\delta_1 = 0.061, \quad \epsilon_1 = 430 \text{ km}, \quad \epsilon_2 = -113 \text{ km}, \quad \epsilon_3 = -9 \text{ km}.$$

IRT - RV at mid mission ($t_0 = t_{mid}$):

$$\delta_1 = -0.290, \quad \epsilon_1 = 28 \text{ km}, \quad \epsilon_2 = -55 \text{ km}, \quad \epsilon_3 = -170 \text{ km}.$$

ET - RV at the beginning ($t_0 = t_{ini}$):

$$\delta_1 = 0.473, \quad \epsilon_1 = 70 \text{ km}, \quad \epsilon_2 = -483 \text{ km}, \quad \epsilon_3 = 42 \text{ km}.$$

ET - RV at mid mission ($t_0 = t_{mid}$):

$$\delta_1 = -0.047 \quad \epsilon_1 = 193 \text{ km}, \quad \epsilon_2 = 52 \text{ km}, \quad \epsilon_3 = 18 \text{ km}.$$

Table 3 provides more results and details for the four cases (2 configurations \times 2 RV times) considered here.

Some results are also plotted in Figure 2 and 3 for IRT and ET configurations, respectively. The ranges of LISA-Earth distances and trailing angles, as well as the initial conditions for the S/Cs are reported in Table 4. We observe that the minimum TA is larger when the RV is at mid mission, but the Δ TA is smaller. In general, breathing angles within the specs of 1.5° , can be obtained at smaller distance from Earth for the ET than the IRT configuration.

Figure 4 shows, in a synoptic way, the results of our optimization procedure with respect to Doppler and breathing angle, vs. the minimum trailing angle TA_0 . By comparing these optimized results with those derived from the simplest model shown in Figure 1, we see that, even considering many more perturbing agents, the optimization manages to reduce both performance indicators by about a factor of 2 at small TA. Again we see that the requirement on the breathing remains the most stringent constraint. However, while complying with keeping the breathing within $\pm 1.5^\circ$, we can address the reduction of flexing following again two opposite strategies: we can set the RV at the beginning of the mission, achieving the lowest values of TA_0 (we have 12.5° for the IRT and 12.1° for the ET), and accept a maximum Δ TA of about 8.5 degrees in both cases. Else, if RV takes place at mid-mission, we must accept larger values of TA_0 (13.9° for the IRT and 13.8° for the ET), but TA will change much less during the mission: Δ TA is less than 4.8 degrees in both cases.

5. Conclusions

We have shown that the choice of heliocentric orbits for LISA is a viable solution even when reducing the arm-length: this allows a substantial reduction in the TA (with deriving beneficial savings for placement in orbit and communications with Earth), of an amount that depends on the assumed mission duration. For an expected mission time of 6 years, the minimum value of the TA can be reduced to about 12° . Should a 2-link interferometer be preferred for a new, cheaper version of the LISA mission, the Isosceles Right Triangle is a viable configuration, as stable as the Equilateral Triangle in all of the tests we have computed. The amount of flexing that the constellation undergoes during the mission depends strongly on the initial conditions. The reasons of this behaviour lie mostly in the time dependent perturbations due to the eccentricity of the Earth orbit and to the motion of the Sun with respect to the Solar System Barycenter. A more detailed analysis of these effects is underway.

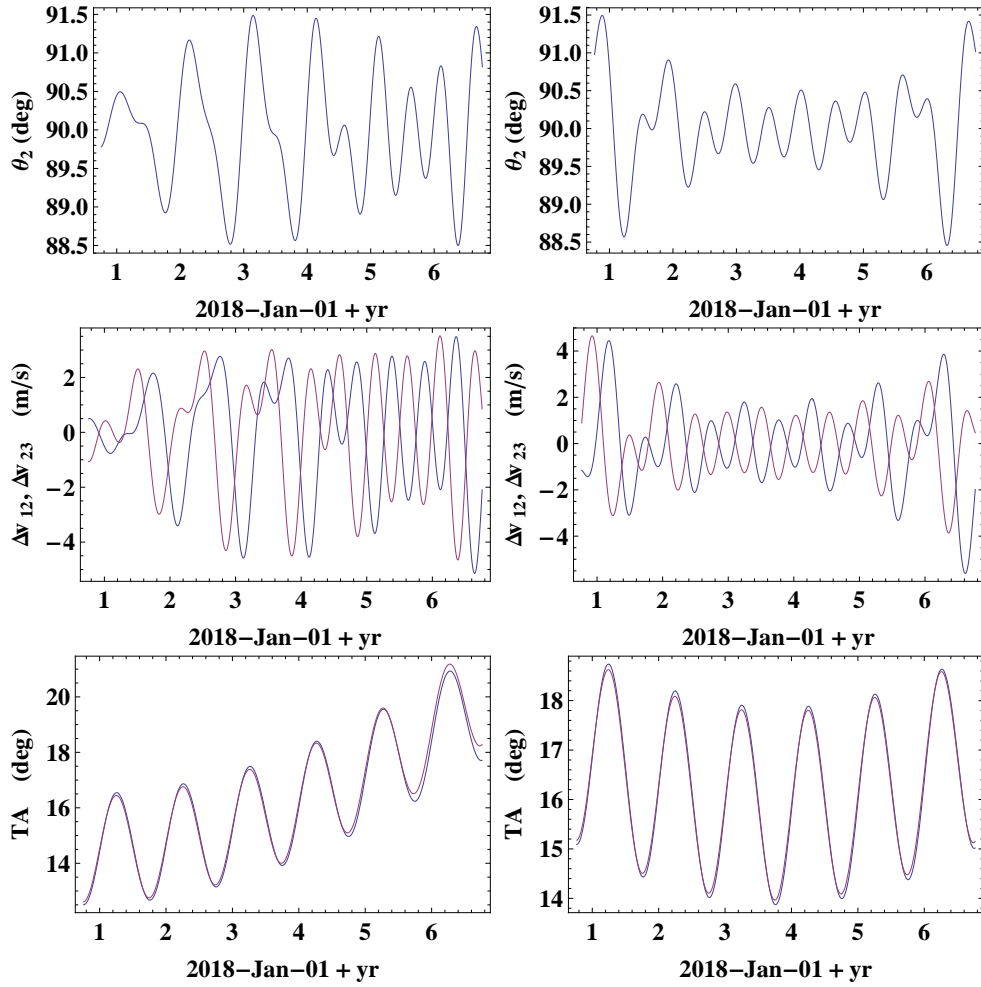


Figure 2: Fully numerical optimization (Section 4.3) with respect to both initial conditions and tilt angle for the IRT configuration. Left panels: RV at the beginning of the mission, right panels: RV at mid-mission. Top panels: breathing angles. Center panels: Doppler shifts. Lower panels: distance LISA-Earth, expressed as TA (red lines are obtained using (B.6)).

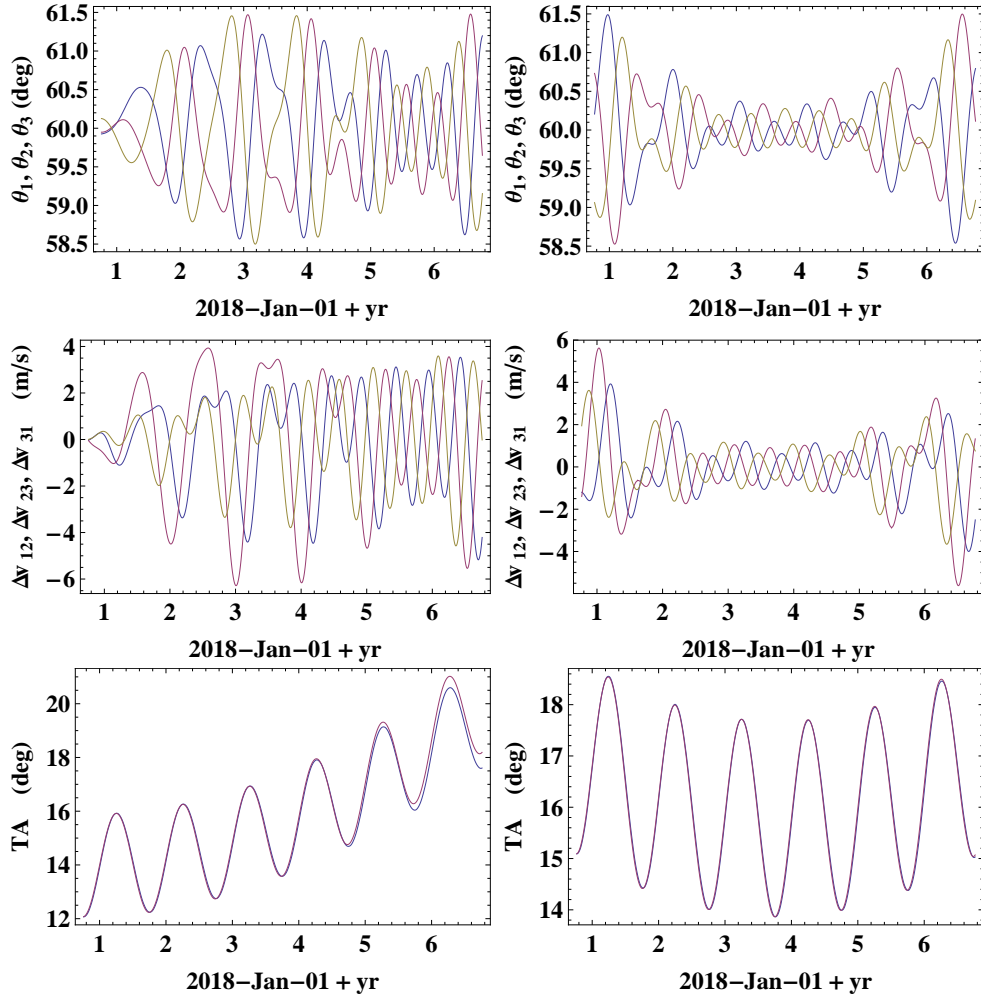


Figure 3: Same as in Figure 2, but for the ET configuration. Left panels: RV at the beginning of the mission, right panels: RV at mid-mission. Top panels: breathing angles. Center panels: Doppler shifts. Lower panels: distance LISA-Earth, expressed as TA (red lines are obtained using (B.6))

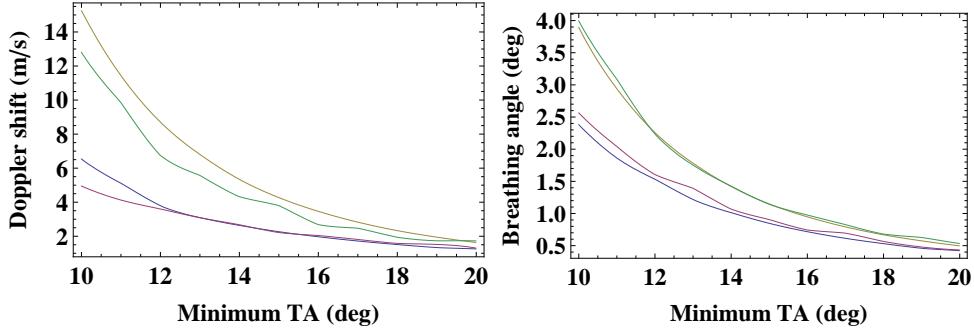


Figure 4: Results of the optimization. Left: maximum Doppler shift in m/s . Right: maximum change of the angle between L_{12} and L_{13} (short arms in the IRT). Red curves: ET (RV at the beginning of the mission), blue curves: IRT (RV at the beginning of the mission), yellow curves: ET (RV at mid mission), green curves: IRT (RV at mid mission).

Table 3: Variation of the same orbital indicators as in Table 1 and 2 (arm length, breathing, Doppler modulation) including the effect of the main bodies of the Solar System for the IRT and ET constellations (left and right, respectively).

RV at t_{ini}	IRT				ET			
	nominal	mean	Δ^+	Δ^-	nominal	mean	Δ^+	Δ^-
L_{12} [km]	10^6	1001798	+19402	-13718	10^6	1000466	+15507	-15009
L_{23} [km]	10^6	1002801	+20096	-11128	10^6	1001006	+27444	-24115
L_{31} [km]	$\sqrt{2} 10^6$	1417361	+17162	-9388	10^6	1001529	+14365	-11594
θ_1 [deg]					60	59.99	+1.45	-1.48
θ_2 [deg]	90	89.99	+1.48	-1.48	60	60.05	+1.21	-1.42
θ_3 [deg]					60	59.94	+1.47	-1.08
$\Delta \mathbf{v}_{12}$ [m/s]	-	-0.07	+3.35	-5.14	-	-0.05	+3.32	-5.17
$\Delta \mathbf{v}_{23}$ [m/s]	-	+0.01	+3.44	-4.62	-	-0.08	+3.91	-6.15
$\Delta \mathbf{v}_{31}$ [m/s]	-				-	+0.03	+3.57	-4.46
distance [Gm]		32.6 \div 54.5				31.4 \div 53.6		
TA [deg]		12.5 \div 21.0				12.1 \div 20.7		
RV at t_{mid}	nominal	mean	Δ^+	Δ^-	nominal	mean	Δ^+	Δ^-
L_{12} [km]	10^6	1002735	+25125	-15193	10^6	1001438	+16132	-14048
L_{23} [km]	10^6	1002580	+17867	-13678	10^6	1001331	+22290	-22441
L_{31} [km]	$\sqrt{2} 10^6$	1418240	+15529	-3942	10^6	1001359	+14976	-10561
θ_1 [deg]					60	59.99	+1.18	-1.12
θ_2 [deg]	90	90.02	+1.49	-1.49	60	60.00	+1.45	-1.45
θ_3 [deg]					60	60.00	+1.46	-1.46
$\Delta \mathbf{v}_{12}$ [m/s]	-	-0.04	+4.44	-5.44	-	-0.02	+3.86	-3.92
$\Delta \mathbf{v}_{23}$ [m/s]	-	+0.06	+4.56	-4.82	-	+0.01	+5.52	-5.55
$\Delta \mathbf{v}_{31}$ [m/s]	-				-	+0.04	+3.60	-3.62
distance [Gm]		36.1 \div 48.6				36.1 \div 48.2		
TA [deg]		13.9 \div 18.7				13.8 \div 18.5		

Table 4: Initial conditions for the IRT (top) and ET (bottom) configuration in the heliocentric reference frame.

	$X(t_0)$ [Gm]	$Y(t_0)$ [km]	$Z(t_0)$ [km]	$\dot{X}(t_0)$ [km/h]	$\dot{Y}(t_0)$ [km/h]	$\dot{Z}(t_0)$ [km/h]
IRT, RV at t_{ini}	$t_{min} = 2018\text{-Oct-05}$					
S/C1	149932288	2412779	612461	1721	106957	0
S/C2	149588968	1697856	2895	1471	107213	438
S/C3	149222635	2401359	609567	1729	107465	0
IRT, RV at t_{mid}	$t_{min} = 2018\text{-Oct-07}$					
S/C1	149753118	2563623	611220	1831	107004	10
S/C2	149404775	1872191	11110	1595	107265	438
S/C3	149042293	2568312	608484	1845	107514	9
ET, RV at t_{ini}	$t_{min} = 2018\text{-Oct-05}$					
S/C1	149884804	553415	500457	395	107017	0
S/C2	149453230	51258	248057	217	107327	311
S/C3	149450059	1052373	248057	576	107326	311
ET, RV at t_{mid}	$t_{min} = 2018\text{-Oct-07}$					
S/C1	149701044	1382500	499337	987	107064	9
S/C2	149267830	902343	257543	824	107378	307
S/C3	149266254	1881003	237763	1167	107370	314

Appendix A. Initial Conditions for the motion in the Earth field.

Equation (8) can be recast in the following, equivalent but more explicit form, where the constants C_{ij} of (7) are folded into the solution:

$$\begin{aligned}
x_k^{(2)} &= x_\oplus + 2A_k + 2y_\oplus\omega t + B_k \cos \omega t + C_k \sin \omega t + \\
&\quad \ell \frac{(C_{11} + 12C_{22}) \cos \sigma_k + 2(2C_{12} + (C_{11} + 4C_{22})\omega t) \sin \sigma_k}{8\sqrt{3}}, \\
y_k^{(2)} &= 4y_\oplus - \left(3\frac{A_k}{2} + 2x_\oplus\right)\omega t - \frac{3}{2}y_\oplus(\omega t)^2 + D_k \\
&\quad + 2(C_k \cos \omega t - B_k \sin \omega t) \\
&\quad - \ell \frac{(3C_{11} + 16C_{22}) \cos \sigma_k - 2(2C_{12} + (C_{11} + 4C_{22})\omega t) \cos \sigma_k}{4\sqrt{3}}, \\
z_k^{(2)} &= E_k \cos \sigma_k + F_k \sin \sigma_k - \frac{\ell}{4}\sigma_k \sin \sigma_k,
\end{aligned}$$

where the σ_k are the time-dependent phases (3).

The 18 constants A_k, \dots, F_k are determined by the initial conditions, that are chosen assuming $(x_k^{(E)}, y_k^{(E)}, z_k^{(E)}) = (0, 0, 0)$ at $t = 0$.

They are:

$$\begin{aligned}
A_k &= -\ell \frac{2C_{22} \cos \sigma_k^0 - C_{12} \sin \sigma_k^0}{\sqrt{3}}, \\
B_k &= -x_\oplus - \frac{\sqrt{3}\ell}{24}((C_{11} - 4C_{22}) \cos \sigma_k^0 + 4C_{12} \sin \sigma_k^0), \\
C_k &= -2y_\oplus + \frac{\sqrt{3}\ell}{24}((C_{11} - 4C_{22}) \sin \sigma_k^0 - 4C_{12} \cos \sigma_k^0), \\
D_k &= \frac{\ell}{2\sqrt{3}}(C_{12} \cos \sigma_k^0 - 2(C_{11} + 3C_{22}) \sin \sigma_k^0), \\
E_k &= -\frac{\ell}{4} \sin^2 \sigma_k^0, \quad F_k = -\frac{\ell}{8} (2\sigma_k^0 - \sin 2\sigma_k^0),
\end{aligned}$$

where the $\sigma_k^0 = \frac{2\pi(k-1)}{n}$ are the relative phase shifts of (3) evaluated at $t = 0$.

Appendix B. Distance Earth-LISA barycenter in epicyclic approximation

Here we calculate the analytic expression for the distance between a particle (i.e.: the LISA barycenter) and the Earth, taking into account the eccentricity of the orbit.

We consider the Earth orbit in epicyclic approximation (at $t = 0$ in the perihelion) in the inertial frame centered in the Sun:

$$\mathbf{R}_\oplus(t) = R_0 \left\{ \cos \omega t + \frac{e}{2} \cos 2\omega t - \frac{3}{2}e, \sin \omega t + \frac{e}{2} \sin 2\omega t, 0 \right\}. \quad (\text{B.1})$$

The LISA barycenter, as a first approximation, can be considered at rest in the HCW frame at TA_0 degrees from the Earth. In the inertial frame its trajectory is

$$\mathbf{R}_g(t) = R_0 \{ \cos(\omega t - \text{TA}_0), \sin(\omega t - \text{TA}_0), 0 \}$$

At zero-order, the force of the Earth on the particle is

$$\mathbf{f} = \epsilon R_0 \omega^2 \{f_x + ec_x \cos \omega t + es_x \sin \omega t, f_y + ec_y \cos \omega t + es_y \sin \omega t, 0\} \quad (\text{B.2})$$

where $e \approx 0.01671$ is the eccentricity of the Earth's orbit and

$$\begin{aligned} \epsilon &= \frac{M_\oplus}{4M_\odot \sqrt{2 - 2 \cos \text{TA}_0}}; & f_x &= -2; & f_y &= \frac{2}{\tan \text{TA}_0/2}; \\ c_x &= \frac{2}{\cos \text{TA}_0 - 1} - 1; & c_y &= \frac{1}{\tan \text{TA}_0/2}; \\ s_x &= \frac{2}{\tan \text{TA}_0/2}; & s_y &= \frac{8}{\cos \text{TA}_0 - 1} + 2. \end{aligned}$$

The new perturbation parameter ($\epsilon = 2.6 \times 10^{-4}$ for $\text{TA}_0 = 10^\circ$) is slightly different from that introduced in (6) to show the explicit dependence on TA_0 . The coefficients ec_x, ec_y, es_x, es_y are much smaller than f_x and f_y and therefore we neglect the terms proportional to $e\epsilon$ in (B.2) and solve perturbatively the HCW equations, assuming $\mathbf{r}_g = \{0, 0, 0\}$ as the unperturbed motion. We calculate the perturbation $\mathbf{r}_1(t)$ with the assumptions $\mathbf{r}_1(t_0) = \{0, 0, 0\}$ and $\dot{\mathbf{r}}_1(t_0) = \{0, 0, 0\}$ where t_0 is the epoch at which we put the particle at TA_0 degrees from the Earth. Letting $t' = t - t_0$ we have

$$\begin{aligned} \mathbf{r}_1(t') &= \epsilon R_0 \{f_x(1 - \cos \omega t') + 2f_y(\omega t' - \sin \omega t'), \\ &\quad 2f_x(\sin \omega t' - \omega t') + f_y(4 - 4 \cos \omega t' - 3/2 \omega^2 t'^2), \\ &\quad 0\} \end{aligned} \quad (\text{B.3})$$

We transform (B.3) in the inertial coordinates using (10) and we calculate the distance $d(t)$ of the particle from the Earth using the expression (B.1). Finally, we expand in Taylor series the distance to the first order in e and ϵ

$$d(t) = d_0 + e d_1(t) + \epsilon d_2(t) + O(e^2) \quad (\text{B.4})$$

where

$$\begin{aligned} d_0 &= R_0 \sqrt{2 - 2 \cos \text{TA}_0} \\ d_1(t) &= \frac{R_0}{\sqrt{2 - 2 \cos \text{TA}_0}} [(\cos \text{TA}_0 - 1) \cos \omega t + 2 \sin \text{TA}_0 \sin \omega t] \\ d_2(t') &= \frac{R_0}{2\sqrt{2 - 2 \cos \text{TA}_0}} \times \\ &\quad \times f_x + 2f_y \omega t' - f_x \cos \text{TA}_0 - 2f_y \omega t' \cos \text{TA}_0 + 1/2(-8f_y + 4f_x \omega t' + \\ &\quad + 3f_y \omega^2 t'^2) \sin \text{TA}_0 + \cos \omega t'(-f_x + f_x \cos \text{TA}_0 + 4f_y \sin \text{TA}_0) + \\ &\quad + (-2f_y + 2f_y \cos \text{TA}_0 - 2f_x \sin \text{TA}_0) \sin \omega t'. \end{aligned}$$

The term d_0 is a constant, the term d_1 is a sum of sinusoids with 1year period. The d_2 term contains linear and quadratic terms in $t - t_0$, and is therefore negligible for $t \approx t_0$ because $\epsilon \ll e$ but it becomes dominant for larger t .

The epochs of the relative minima and maxima of $d(t)$ depend on TA_0 but not on t_0 . They are found by equating to zero the first derivative of d_1 :

$$2 \cos \omega t \sin \text{TA}_0 + (1 - \cos \text{TA}_0) \sin \omega t = 0.$$

With the additional condition on the second derivative

$$(1 - \cos TA_0) \cos \omega t_{min} - 2 \sin TA_0 \sin \omega t_{min} > 0,$$

the minima occur at

$$t_{min,k} = -\frac{1}{\omega} \arctan \left[\frac{2}{\tan(TA_0/2)} \right] + \frac{2k\pi}{\omega}, \quad k \in \mathbb{Z}. \quad (\text{B.5})$$

In the same fashion of (B.4), the TA can be obtained, to first order in e , as

$$TA(t) = TA_0 + 2e \sin \omega t + \epsilon \left[4f_y(\cos \omega t' - 1) + 2f_x(\omega t' - \sin \omega t') + \frac{3}{2}f_y(\omega t')^2 \right]. \quad (\text{B.6})$$

Although the epochs t_{min} are obtained using a first-order approximation, they are in good agreement with the exact values (for an example, see the bottom panels of Figure 2 and 3).

Acknowledgments

We thank Oliver Jennrich, Pete Bender and Bill Weber for useful discussions.

References

- [1] Bik J J C M, Visser P N A M and Jennrich O 2007, *Advances in Space Research* **40**, 25.
- [2] Nerem S 2003, <http://ccar.colorado.edu/asen5050/lecture12.pdf>
- [3] Rajesh Nayak K, Koshti S, Dhurandhar S V and Vinet J-Y 2006, *Class. Quantum Grav.* **23**, 1763.
- [4] Sweetser T H 2005, Epicycles and oscillations: the dynamics of the LISA orbits, paper AAS 05-292, AAS/AIAA Astrodynamics Specialist Conference.
- [5] Dhurandhar S V, Rajesh Nayak K, Koshti S and Vinet J-Y 2005, *Class. Quantum Grav.* **22**, 481.
- [6] Pucacco G, Bassan M and Visco M 2010, *Class. Quantum Grav.* **27**, 235001.
- [7] Dhurandhar S V, Rajesh Nayak K and Vinet J-Y 2008, *Class. Quantum Grav.* **25**, 245002.
- [8] Hughes, S P 2005, Preliminary optimal orbit design for LISA, *25th Annual AAS Guidance and Control Conference*.
- [9] Xia Y, Li G Y, Heinzel G, Rüdiger A and Luo Y J 2010, *Sci. China Phys. Mech. Astron.* **53**, 179.
- [10] Li G, Yi Z, Heinzel G, *et al.* 2008, *Int J Mod Phys D*, **17**, 1021-1042.
- [11] Cerdonio M, De Marchi F, De Pietri R, Jetzer P, Marzari F, Mazzolo G, Ortolan A and Sereno M 2010, *Class. Quantum Grav.* **27**, 165007.
- [12] <http://ssd.jpl.nasa.gov/horizons.cgi>